X-ray magnetic circular dichroism of ferromagnetic Co4N epitaxial films on SrTi03(001) substrates grown by molecular beam epitaxy

doi: 10.1063/1.3670353

X-ray magnetic circular dichroism of ferromagnetic Co_4N epitaxial films on $SrTiO_3(001)$ substrates grown by molecular beam epitaxy

Keita Ito,[1] Kazunori Harada,[1] Kaoru Toko,[1] Mao Ye,[2] Akio Kimura,[2] Yukiharu Takeda,[3] Yuji Saitoh,[3] Hiro Akinaga,[4] and Takashi Suemasu[1,a)]
[1]*Institute of Applied Physics, University of Tsukuba, Ibaraki 305-8573, Japan*
[2]*Graduate School of Science, Hiroshima University, Hiroshima 739-8526, Japan*
[3]*Japan Atomic Energy Agency (JAEA), SPring-8, Hyogo 679-5198, Japan*
[4]*National Institute of Advanced Industrial Science and Technology (AIST), Ibaraki 305-8569, Japan*

(Received 1 October 2011; accepted 27 November 2011; published online 19 December 2011)

5-nm thick Co_4N layers capped with 3-nm thick Au layers were grown epitaxially on $SrTiO_3(001)$ substrates by molecular beam epitaxy using solid Co and a radio-frequency NH_3 plasma. Spin and orbital magnetic moments of the Co_4N layers were estimated using x-ray magnetic circular dichroism (XMCD) measurements at 300 K. The site-averaged Co 3*d* spin magnetic moment is evaluated to be about 1.4 μ_B, which is smaller than that predicted theoretically (1.58 μ_B). The element-specific XMCD intensities for the Co L_3 edge and N *K* edge show that the magnetic moment is induced at the N atoms. © *2011 American Institute of Physics*. [doi:10.1063/1.3670353]

Ferromagnetic iron nitrides are composed of abundant and nontoxic elements and have been subjected to extensive research for applications in magnetic recording devices. In particular, the spin polarization of electrical conductivity $[P_\sigma = (\sigma_\uparrow - \sigma_\downarrow)/(\sigma_\uparrow + \sigma_\downarrow)]$ at the Fermi level is theoretically predicted to be −1.0 in Fe_4N.[1] In addition, an inverse magnetoresistance ratio of −75% was reported at room temperature (RT) in CoFeB/MgO/Fe_4N magnetic tunnel junctions.[2] Recent spin polarization measurements of P_σ by point-contact Andreev reflection and magnetic moments obtained using x-ray magnetic circular dichroism (XMCD) show that Fe_4N is considered to be an appropriate material for application in spintronics devices.[3,4] Very recently, the spin polarization of the density of states $[P_{DOS} = (D_\uparrow - D_\downarrow)/(D_\uparrow + D_\downarrow)]$ at the Fermi level in Co_4N was theoretically predicted to be larger (−0.88) than that in Fe_4N (−0.67).[5] Co_4N has the same cubic perovskite lattice structure as Fe_4N, where a N atom is located at the body center of a fcc-Co unit cell. There have been a few reports on first-principles calculations of magnetic moments at each Co site in a Co_4N unit cell.[5,6] According to these, the magnetic moments of Co atoms at corner and face-centered sites, namely Co(I) and Co(II), are approximately 2.0 and 1.5 μ_B, respectively. The magnetic moment of N atom is calculated to be approximately 0.07 μ_B. However, there have been only a few reports on the growth of single phase Co_4N bulk and films.[7,8] Thus, the magnetic properties of Co_4N have yet to be evaluated. In this work, we have grown Co_4N layers epitaxially on $SrTiO_3$(STO)(001) substrates by molecular beam epitaxy (MBE) using solid Co and a radio-frequency (RF) NH_3 plasma.[9] We have already demonstrated growth of Fe_4N epitaxial films using the same technique.[10] XMCD measurements were performed for the Co_4N epitaxial film, and the spin and orbital magnetic moments of Co_4N were deduced. There have been no reports thus far on the magnetic moments of Co_4N using XMCD measurements.

Au(3 nm)/Co_4N(5 nm)/STO(001) (sample A) was grown at 450 °C using 3N-Co and RF-NH_3. After growth of the 5-nm-thick Co_4N layer, a 3-nm-thick Au capping layer was subsequently deposited at RT in the same MBE chamber to prevent oxidation of the surface. We also prepared Au(3 nm)/hcp-Co(5 nm)/MgO(001) (sample B) by MBE as a reference sample. The hole number of the Co 3*d* orbit (N_h) in hcp-Co is known to be 2.49.[11] X-ray absorption spectroscopy (XAS) and XMCD spectra at Co $L_{2,3}$ edges for samples A and B were measured using the total electron yield method at the BL23SU of the SPring-8 facility in Japan. Circularly polarized x-rays were incident perpendicular to the sample surface with an external magnetic field (*H*) applied perpendicular to the sample surface. We confirmed that the magnetic moments of samples A and B were saturated at 300 K under $H = 4$ T. In addition, the *H* dependence of element-specific XMCD signals were measured with the same experimental geometry and temperature at the Co L_3 (778.25 eV) and N *K* (396.4 eV) absorption edges for sample A.

Figure 1 shows (a) XAS and (b) XMCD spectra at the Co $L_{2,3}$ absorption edges of samples A and B measured at 300 K. The signals were averaged between those measured under an external *H* of +4 T and −4 T. Clear MCD signals are observed in both samples. If cobalt oxides are contained in these samples, the XAS spectrum at Co $L_{2,3}$ edges is likely to split into a multiplet.[12] There are no multiplet peaks observed in the present XAS spectra of samples A and B, indicating that the surfaces of these samples are not oxidized. A small shoulder structure is observed on the higher energy side of the Co L_3 absorption edge for sample A. The similar feature has also been reported for the Fe L_3 absorption spectrum of Fe_4N.[4,13] Here, we interpret that the observed shoulder structure originates from different chemical bonding at inequivalent 3*d* metal sites, which are characteristic of 3*d* metal perovskite nitrides.

Spin and orbital magnetic moments of samples A and B were deduced by applying magneto-optical sum-rules analysis.[11,14,15] The backgrounds of the XAS spectra were removed by subtracting the two step function from the raw

a)Author to whom correspondence should be addressed. Electronic mail: suemasu@bk.tsukuba.ac.jp.

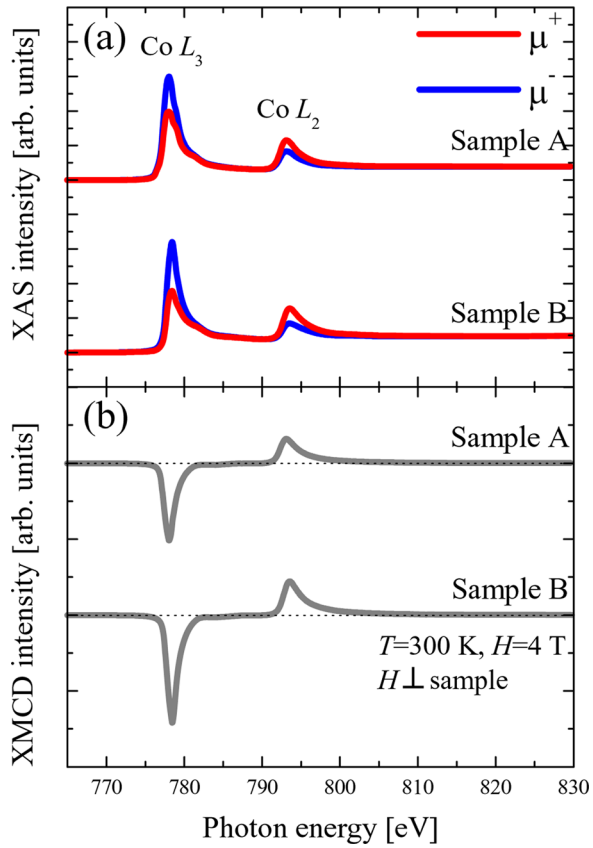

FIG. 1. (Color online) (a) XAS and (b) XMCD spectra at the Co $L_{2,3}$ edges of samples A and B observed at 300 K. The external magnetic field ($H = \pm 4$ T) was applied perpendicular to the sample surface.

XAS spectra. The N_h of the Co 3*d* orbital in sample A (Co_4N) was determined to be approximately 2.51 from the XAS spectra of samples A and B by referring to the N_h value in hcp-Co (2.49).[11] The N_h value of the Fe 3*d* orbital in Fe_4N was also deduced using the same procedure as in Ref. 13. The orbital, spin, and total magnetic moments of samples A and B are summarized in Table I. The reported values of the magnetic moments of Co_4N and hcp-Co are also shown for comparison.[5,6,9,16] The orbital and spin magnetic moments of sample A were evaluated to be $0.06 \pm 0.01\ \mu_B$ and $1.31 \pm 0.11\ \mu_B$ per Co atom, respectively. The deduced spin magnetic moment is smaller than that of the theoretically predicted value of $1.58\ \mu_B$.[5] The site-averaged magnetic moment summed over spin and orbital components was $1.37 \pm 0.12\ \mu_B$ per Co atom. This value is also smaller than that measured ($1.6\ \mu_B$, 1300 emu/cc) using a superconducting quantum interface device magnetometer (SQUID) at RT.[9] It is known that the sum-rule analysis for the XMCD experiment in the total electron yield mode underestimates the magnetic moments. The orbital and spin magnetic moments of sample B were evaluated to be $0.09 \pm 0.01\ \mu_B$ and $1.76 \pm 0.13\ \mu_B$ per Co atom, respectively. In case that the light is incident normal to the film plane with Co film thickness of 5 nm, the fractions of the values for orbital and spin moments are 0.76 and 0.93 with respect to the ideal values, respectively.[17] Using these correction factors for sample B, the orbital and spin magnetic moments are corrected to be as 0.12 and $1.89\ \mu_B$, respectively, which are close to those reported by neutron diffraction for hcp-Co.[16] The correction should be made for samples with thickness larger than the probing depth in the total electron yield mode.[17] Although the probing depth for Co is not clear, this correction for Co seems appropriate in this case. The film thickness of sample A is the same as in sample B. We assume here that there is no significant difference in probing depth between Co and Co_4N. Thus, the correction is also necessary for Co_4N although there have been no data thus far on the correction factors for this material. We thus obtain the corrected values of orbital and spin magnetic moments of sample A as 0.08 and $1.40\ \mu_B$, respectively, which are closer to but are still smaller than those obtained from the calculation and the saturation magnetization.[5,6,9]

Figure 2 shows (a) XAS and (b) XMCD spectra at the N *K* absorption edge of sample A measured at 300 K. Several peaks were observed in the XAS spectrum as shown in Fig. 2(a). The N *K* edge spectrum shows a sharp peak at 396 eV followed by two broad features at 398 and 399 eV. Another absorption starts from the photon energy of 404 eV. Among these features, a distinct MCD signal is observed at the lowest energy peak position, whereas no dichroism is found for the others. This trend is the same as that reported in the XMCD spectrum of Fe_4N at the N *K* edge,[18] implying that the magnetic moment is induced at the N sites. By comparing the present result at N *K* edge with the predicted density of states in Ref. 6, we can interpret that the first absorption peak at 396 eV arises from the optical transition from N 1*s* to unoccupied N 4*p* orbital strongly hybridized with Co(II) 3*d* minority spin state.

TABLE I. Orbital, spin, and total magnetic moments of Co_4N and hcp-Co deduced by experimental and theoretical analyses. Corrected moment values of samples after taking the saturation effect into account are listed in parentheses.

Compounds	Magnetic moment [μ_B per Co atom]			Method	Reference
	m_{orb}	m_{spin}	m_{total}		
Co_4N/STO	0.06 ± 0.01	1.31 ± 0.11	1.37 ± 0.12	XMCD	This work
(corrected)	(~0.08)	(~1.40)	(~1.48)		
hcp-Co/MgO	0.09 ± 0.01	1.76 ± 0.13	1.84 ± 0.14	XMCD	This work
(corrected)	(~0.12)	(~1.89)	(~2.01)		
Co_4N	—	1.58	—	Theory	5
Co_4N	—	1.60	—	Theory	6
Co_4N	—	—	1.6	SQUID	9
hcp-Co	0.13 ± 0.01	1.86 ± 0.07	1.99 ± 0.08	Neutron diffraction	16

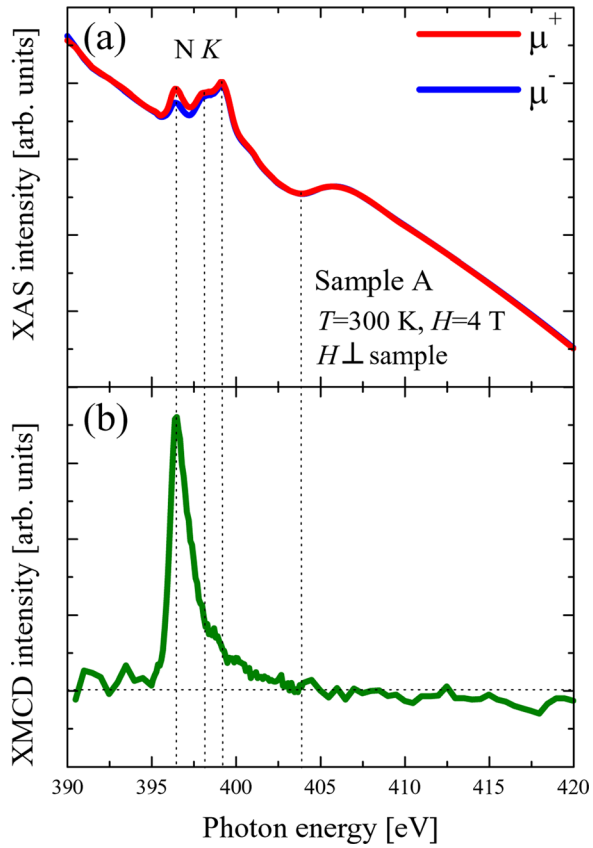

FIG. 2. (Color online) (a) XAS and (b) XMCD spectra at the N *K* absorption edge of sample A observed at 300 K. The external magnetic field ($H = \pm 4$ T) was applied perpendicular to the sample surface.

Figure 3 shows the H dependence of element-specific XMCD signals for the Co L_3 edge and N K edge of sample A measured at 300 K. The XMCD signals at the N K edge are very weak. However, we have confirmed that the XMCD intensity for N atoms follows that of Co atoms and is saturated under the same external H of approximately ± 2 T. This result indicates that the magnetic moment is induced at the N atoms, probably by band hybridization between Co and N atoms. Interestingly, the sign of the MCD signal for the N K edge is opposite to that for the Co L_3 edge. Note that the corresponding sign was the same between the Fe L_3 edge and N K edge in Fe_4N.[4] The origin of this difference currently remains an open question. Further theoretical studies are required to address this issue.

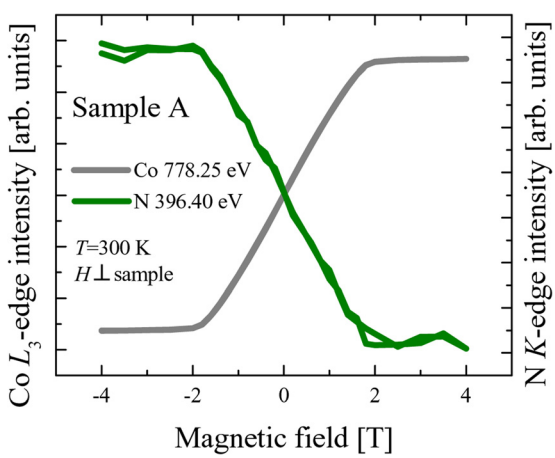

FIG. 3. (Color online) H dependence of element-specific XMCD intensities for Co and N atoms in sample A measured at 300 K. The external magnetic field was applied perpendicular to the sample surface.

In summary, we deduced the orbital and spin magnetic moments of the MBE-grown Co_4N(5 nm)/STO(001) epitaxial film using XMCD measurements. The orbital and spin magnetic moments of Co_4N were evaluated to be $0.06 \pm 0.01\ \mu_B$ ($\sim 0.08\ \mu_B$) and $1.31 \pm 0.11\ \mu_B$ ($\sim 1.40\ \mu_B$) per Co atom before (after) considering the saturation effect, respectively. These values are smaller than those of hcp-Co. The element-specific XMCD intensities for the Co L_3 edge and N K edge imply that the magnetic moment is induced at the N atoms.

This work was supported in part by a Grant-in-Aid for Scientific Research on the Priority Area of "Creation and Control of Spin Current" (19048030) from the Ministry of Education, Culture, Sports, Science and Technology of Japan (MEXT) and by the NanoProcessing Partnership Platform (NPPP) at AIST, Tsukuba. XMCD measurements were performed at SPring-8 BL23SU under Nanonet Support Proposals (2011A3872). The authors also thank Dr. N. Ota and Professor K. Asakawa of the Tsukuba Nano-Tech Human Resource Development Program at the University of Tsukuba for useful discussions.

[1]S. Kokado, N. Fujima, K. Harigaya, H. Shimizu, and A. Sakuma, Phys. Rev. B **73**, 172410 (2006).
[2]Y. Komasaki, M. Tsunoda, S. Isogami, and M. Takahashi, J. Appl. Phys. **105**, 07C928 (2009).
[3]A. Narahara, K. Ito, T. Suemasu, Y. K. Takahashi, A. Rajanikanth, and K. Hono, Appl. Phys. Lett. **94**, 202502 (2009).
[4]K. Ito, G. H. Lee, K. Harada, M. Suzuno, T. Suemasu, Y. Takeda, Y. Saitoh, M. Ye, A. Kimura, and H. Akinaga, Appl. Phys. Lett. **98**, 102507 (2011).
[5]Y. Imai, Y. Takahashi, and T. Kumagai, J. Magn. Magn. Mater. **322**, 2665 (2010).
[6]S. F. Matar, A. Houari, and M. A. Belkhir, Phys. Rev. B **75**, 245109 (2007).
[7]N. Terao, Mem. Sci. Rev. Met. **57**, 96 (1960).
[8]K. Oda, T. Yoshio, and K. Oda, J. Mater. Sci. **22**, 2729 (1987).
[9]K. Ito, K. Harada, K. Toko, H. Akinaga, and T. Suemasu, J. Cryst. Growth **336**, 40 (2011).
[10]K. Ito, G. H. Lee, H. Akinaga, and T. Suemasu, J. Cryst. Growth **322**, 63 (2011).
[11]C. T. Chen, Y. U. Idzerda, H. J. Lin, N. V. Smith, G. Meigs, E. Chaban, G. H. Ho, E. Pellegrin, and F. Sette, Phys. Rev. Lett. **75**, 152 (1995).
[12]H. Liu, J. Guo, Y. Yin, A. Augustsson, C. Dong, J. Nordgren, C. Chang, P. Alivisatos, G. Thornton, D. F. Ogletree, F. G. Requejo, F. D. Groot, and M. Salmeron, Nano. Lett. **7**, 1919 (2007).
[13]Y. Takagi, K. Isami, I. Yamamoto, T. Nakagawa, and T. Yokoyama, Phys. Rev. B **81**, 035422 (2010).
[14]B. T. Thole, P. Carra, F. Sette, and G. van der Laan, Phys. Rev. Lett. **68**, 1943 (1992).
[15]P. Carra, B. T. Thole, M. Altarelli, and X. D. Wang, Phys. Rev. Lett. **70**, 694 (1993).
[16]C. G. Shull and Y. Yamada, J. Phys. Soc. Jpn. **17**(Suppl. BIII), 1 (1962).
[17]R. Nakajima, J. Stöhr, and Y. U. Idzerda, Phys. Rev. B **59**, 6421 (1999).
[18]C. S. Hanke, R. G. Arrabal, J. E. Prieto, E. Andrzejewska, N. Gordillo, D. O. Boerma, R. Loloee, J. Skuza, and R. A. Lukaszew, J. Appl. Phys. **99**, 08B709 (2006).